

DOI: 10.1002/cmdc.200700160

Multispecificity of Drug Transporters: Probing Inhibitor Selectivity for the Human Drug Efflux Transporters ABCB1 and ABCG2

Joerg Cramer,^[c] Stephan Kopp,^[a] Susan E. Bates,^[d] Peter Chiba,^{*[a]} and Gerhard F. Ecker^{*[b]}

Multidrug resistance transporters P-glycoprotein/ABCB1 and ABCG2 limit the effect of a large number of cytostatic and cytotoxic drugs by energy-dependent efflux. In experimental models, pump inhibitors reestablish sensitivity towards these drugs. Both transporters demonstrate remarkably broad and partly overlapping substrate specificity. Propafenone analogues are inhibitors of a large number of drug efflux pumps including P-glycoprotein and ABCG2 as well as the microbial pumps. Here the two human

ABC transporters ABCB1 and ABCG2 have been studied with respect to interaction with this class of compounds. Data indicate that within the same chemical scaffold, selectivity indices span three orders of magnitude. Compounds with the highest selectivity indices contain a non-ionizable nitrogen atom. Qualitative and quantitative pharmacophore models indicate that hydrophobicity, the number of rotatable bonds, and the number of H-bond acceptors are key features for both activity and selectivity.

Introduction

ATP-binding cassette (ABC) transporters are present in all living organisms. The functionally active form of the transporters is composed of two highly conserved motor domains (nucleotide binding domains, NBDs) and two transmembrane domains (TMDs), which are responsible for solute binding and transport. These four domains are either present in one single polypeptide chain (full transporters), or alternatively are expressed as half transporters. In the latter case, ABC transporters need to dimerize to be functionally active. In humans, 48 ABC genes have been identified. Members of this group of membrane proteins have been shown to be involved in a variety of human diseases.^[1]

Particular interest has been attracted by members of the multidrug ABC transporter subfamily, which, in addition to their physiological role in tissue protection, actively extrude a large variety of therapeutically administered drugs from malignant cells and thus have been postulated to cause poor treatment outcome in cancer patients. The three major multidrug resistance ABC proteins are ABCB1 (P-glycoprotein, P-gp),^[2] ABCC1 (multidrug resistance protein 1, MRP1),^[3] and ABCG2 (breast cancer related protein, BCRP).^[4] ABCB1/P-gp is not only overexpressed in human tumor cells but is also physiologically present in a number of tissues such as intestinal epithelial cells, on the canalicular side of hepatocytes and in capillary endothelial cells that form the blood–brain barrier. Hence it interferes with oral drug absorption, drug delivery to the brain and enhances renal and biliary drug excretion. ABCB1/P-gp has therefore attracted considerable attention as an antitarget. ABCG2 is also expressed in human tumor cells and is also considered to serve a physiological role in the intestine.

A hallmark of multispecific drug transporters is the capacity to recognize potentially lethal environmental toxins. The ability of a single protein to engage with multiple ligands offers a means for expanding the repertoire of xenotoxin recognition and for increasing coverage of the chemical space that these natural toxins explore. Multispecificity also plays an important role for the adaptive immune system and the cytochrome P450 system. Three general mechanisms for multispecific ligand recognition have been described. The first is an interaction with an essentially rigid binding pocket providing different interaction sites with structurally distinct ligands.^[5] Alternatively, the protein might possess a variable degree of conformational flexibility that allows it to reconfigure its binding pocket to accommodate structurally diverse ligands by induced fit.^[6] A recent addition to these two concepts is the demonstration that one and the same ligand may bind to a protein in different poses. This phenomenon has been termed “differential

[a] S. Kopp, Prof. Dr. P. Chiba
Institute of Medical Chemistry, Medical University of Vienna
Währinger Strasse 10, 1090 Wien (Austria)
Fax: (+43) 1-4277-60889

[b] Prof. Dr. G. F. Ecker
Department of Medicinal Chemistry, University of Vienna
Althanstrasse 14, 1090 Wien (Austria)
Fax: (+43) 1-4277-9551
E-mail: gerhard.f.ecker@univie.ac.at

[c] Dr. J. Cramer
BioChemInformatics, Intervet Innovation GmbH
Zur Probstei, 55270 Schwabenheim (Germany)

[d] Dr. S. E. Bates
Medical Oncology Branch, National Cancer Institute
Building 10, 10 Center Drive, Bethesda, MD 20892 (USA)

ligand positioning".^[7] The essential feature of this concept is that a single ligand might be bound to spatially distinct regions of the binding site. In principle a given protein may employ various combinations of these strategies to maximize the number and diversity of ligands it recognizes. In the case of P-gp, available evidence suggests that binding occurs in a large hydrophobic pocket, which possesses a significant degree of conformational flexibility that allows reconfiguration in order to accommodate diverse ligands. Whether one specified ligand can bind to multispecific efflux pumps in various positions is presently unknown. In this case, however, consistent results for quantitative structure–activity relationship (SAR) studies should not be obtained. Previous studies on P-gp showed that QSAR studies generate meaningful hypotheses that extend beyond the chemical space of the training set.^[8] Three-dimensional models with distinct pharmacophores including space-directed hydrogen bonding and aromatic features have also been obtained.^[9]

The present study was undertaken to characterize similarities and differences in the ligand recognition pattern of ABCB1 and ABCG2 using a library of propafenone analogues. Furthermore, the question was addressed if these differences can be exploited for the design of inhibitors with increased specificity for one or the other transporter. Our results demonstrate that within the structural scaffold of propafenones, selectivity indices span more than three orders of magnitude.

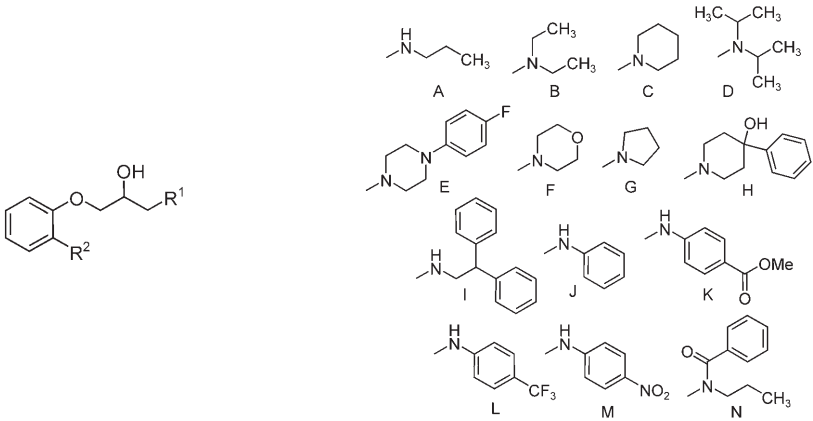
Results and Discussion

Multispecificity remains a challenging issue in drug discovery, because of related drug safety and toxicology issues. An understanding of the molecular basis of interaction of drugs with promiscuous proteins attracts considerable interest, because side effects related to antitargets such as multispecific drug efflux transporters, the hERG potassium channel, the cytochrome P450 family members, and certain G-protein-coupled receptors often lead to late-stage failure of drugs in clinical development.^[10] Two multispecific drug efflux pumps with overlapping substrate specificity, ABCB1 and ABCG2, were chosen to investigate the possibility of the

design of selective inhibitors for one or the other transporter. Analogues of the lead compound propafenone, a class-1c antiarrhythmic agent, have been identified as inhibitors and substrates of the human multidrug transporters ABCB1 (P-gp).^[11] Orthologous microbial efflux pumps, including the bacterial MDR transporter LmrA^[12] and the fungal ABC transporter Pdr5p^[13] are also inhibited by propafenones. This makes them a suitable substance class for the study of the influence of structural modification on selectivity for individual MDR transporters. Extensive prior quantitative SAR studies on P-gp^[14] have formed the basis of the present selectivity profiling study comparing ABCB1 and ABCG2.

Twenty-three compounds, including the lead compound propafenone, were selected from our in-house library on the basis of diversity of their SAR pattern with respect to ABCB1. The chemical structures of these analogues are depicted in Table 1. The set of compounds are modified in the phenone substructure and in the vicinity of the nitrogen atom.

Table 1. General structure of propafenone-type inhibitors.



Compd	R ¹	R ²	log P	EC ₅₀ [μM]		SI (B1/G2)
				ABCB1	ABCG2	
1a	A	COCH ₂ CH ₂ Ph	3.39	1.51	37.9	0.040
1b	B	COCH ₂ CH ₂ Ph	3.62	1.70	33.5	0.051
1c	C	COCH ₂ CH ₂ Ph	3.67	0.80	30.7	0.026
1d	D	COCH ₂ CH ₂ Ph	4.25	0.65	36.4	0.018
1e	F	COCH ₂ CH ₃	2.07	113	440	0.257
1f	E	COCH ₂ CH ₂ Ph	4.93	0.27	4.62	0.058
1g	G	COCH ₂ CH ₂ Ph	2.80	3.60	47.1	0.076
1h	F	COCH ₂ CH ₂ Ph	2.54	5.83	34.0	0.171
1i	C	CH(OCH ₃)CH ₂ CH ₂ Ph	4.30	0.53	12.9	0.041
1j	E	CH(OCH ₃)CH ₂ CH ₂ Ph	5.56	0.09	13.9	0.006
1k	D	CH(OCH ₃)CH ₂ CH ₂ Ph	4.88	0.65	15.2	0.043
1l	E	COPh	4.57	0.79	14.1	0.056
1m	C	CH ₂ Ph	4.20	1.56	31.9	0.049
2a	H	COCH ₃	1.73	1.79	600	0.003
2b	H	COCH ₂ CH ₃	2.38	0.68	58.8	0.012
2c	H	COPh	3.62	0.16	98.3	0.002
3	I	COCH ₂ CH ₂ Ph	6.16	0.39	3.30	0.118
4	D	CH(OH)CH ₂ CH ₂ Ph	4.52	3.01	37.3	0.081
5a	J	COCH ₂ CH ₂ Ph	4.23	5.50	4.21	1.306
5b	K	COCH ₂ CH ₂ Ph	4.05	9.61	1.50	6.407
5c	L	COCH ₂ CH ₂ Ph	5.15	17.3	3.81	4.541
5d	M	COCH ₂ CH ₂ Ph	4.26	7.14	1.24	5.758
6	N	COCH ₂ CH ₂ Ph	4.93	4.47	3.68	1.215

Comparison of EC₅₀ values in ABCB1- and ABCG2-overexpressing cell lines

In an initial set of experiments, the potencies of these substances were evaluated in mitoxantrone accumulation studies with cell lines overexpressing either ABCB1 or ABCG2. Potencies determined in P-gp-expressing CCRFvcr1000 and ABCG2-transfected HEK cells are listed in Table 1 and are correlated with calculated log*P* values in Figure 1 a and b. In P-gp-expressing cells (Figure 1 a) the SAR pattern observed with mitoxantrone is similar to that previously found for daunomycin as substrate. In addition, an identical pattern was observed for HEK-293 cells that were stably transfected to overexpress P-gp (data not shown). This rules out any non-P-gp-related effects on the pharmacological activity of compounds. The lead compound propafenone (1 a) as well as analogues with a tertiary amino group (compounds 1 b–m) showed a good linear correlation

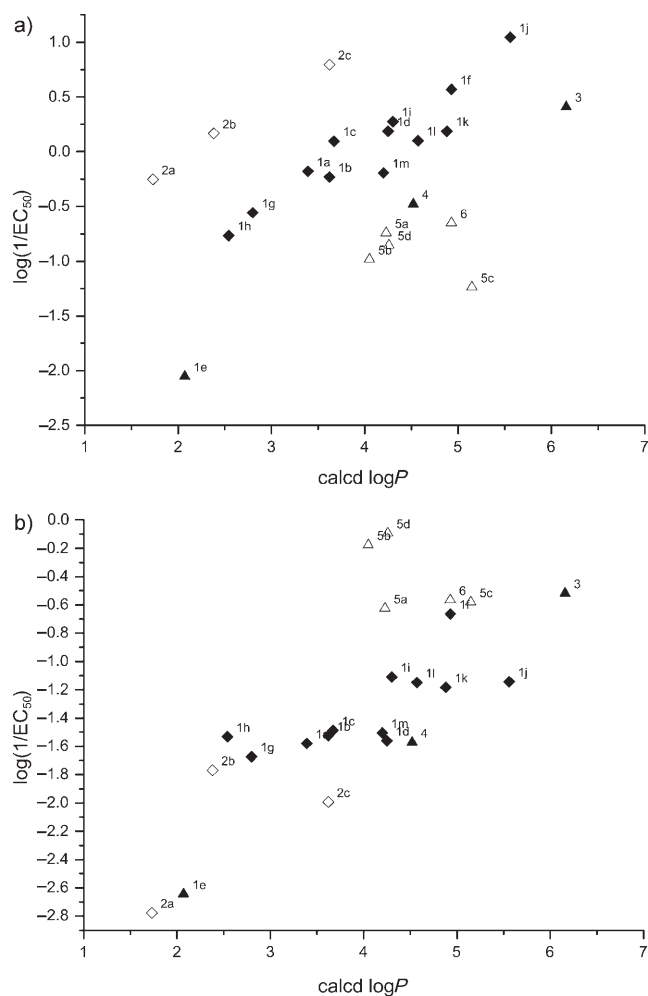


Figure 1. a) Correlation of calculated log*P* and log potency values of propafenone analogues in ABCB1-expressing cells. Tertiary propafenone analogues **1 a–d**, **1 f–m** (◆); 4-phenyl-4-hydroxy-substituted analogues **2 a–c** (◇); compounds **1 e**, **3**, **4** (▲); anilines **5 a–d** and amide **6** (△). b) Correlation of calculated log*P* and log potency values of propafenone analogues in ABCG2-expressing cells. Tertiary propafenone analogues **1 a–d**, **1 f–m** (◆); 4-phenyl-4-hydroxy-substituted analogues **2 a–c** (◇); compounds **1 e**, **3**, **4** (▲); anilines **5 a–d** and amide **6** (△).

with calculated log*P* values. The 4-hydroxy-4-phenyl-piperidines **2 a–c** showed a 10-fold greater activity than expected on the basis of lipophilicity, whereas the diphenylethylamino analogue **3**, the hydroxy derivative **4**, the anilines **5 a–d**, and the acid amide **6** had between 10- and 100-fold lower activities. Compound **1 e**, which lacks a second aromatic ring system, also showed lower activity than expected. In contrast, the lipophilicity/potency plot for ABCG2 showed a distinctly different picture. Most interestingly, anilines and the amide showed higher log potency/log*P* ratios than expected (Figure 1 b), encouraging considerations with respect to selectivity profiling. Selectivity indices (SI) representing the ABCB1/ABCG2 ratio of EC₅₀ values ranged between 0.002 and 10 (Figure 2). An SI of 1

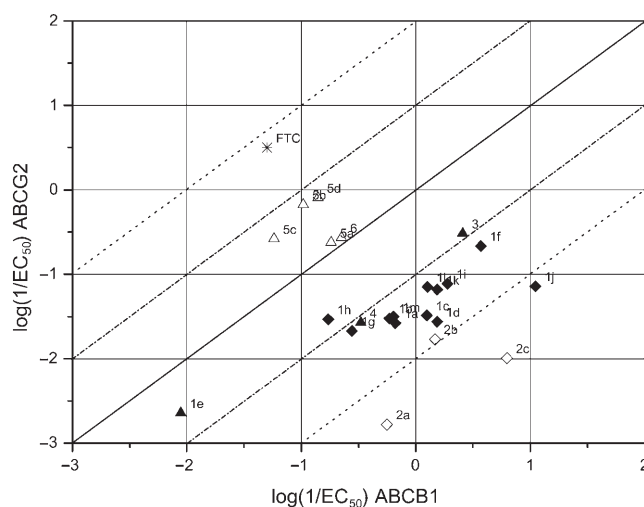


Figure 2. Correlation of log potency values of propafenone analogues and funitremorgin C (FTC) in ABCB1- and ABCG2-expressing cells. Tertiary propafenone analogues **1 a–d**, **1 f–m** (◆); 4-phenyl-4-hydroxy-substituted analogues **2 a–c** (◇); compounds **1 e**, **3**, **4** (▲); anilines **5 a–d** and amide **6** (△); FTC (*). The diagonal line conforms to SI = 1. From left to right, dashed lines correspond to SIs of 100, 10, 0.1, and 0.01.

indicates an equipotent effect on both transporters; if SI > 1, selectivity is for ABCG2, and with SI < 1, selectivity is for ABCB1. In the group of tertiary amines, 4-hydroxy-4-phenylpiperidine-substituted compounds **2 a–c** (◇) showed the highest SIs (0.0016 for **2 c**, 0.0030 for **2 a**, and 0.011 for **2 b**). Other tertiary amines (◆) had selectivity indices between 0.018 and 0.26, indicating higher activity for ABCB1 than for ABCG2. Three compounds (**5 b–d**) were approximately fivefold, and two others, **5 a** and **6**, were slightly more selective for ABCG2 than for ABCB1 (△, SIs in the range of 1.21–6.41). As a control, funitremorgin C (FTC, *), a specific ABCG2 inhibitor,^[15] is also shown. As expected, this substance was greater than two orders of magnitude more selective for ABCG2 (SI = 147).

Role of the nitrogen atom for activity/selectivity

Under physiological pH conditions the nitrogen atom of anilines and amides is predominantly uncharged. Average SIs for tertiary amines (0.062 ± 0.064) differed significantly from those

for anilines and the amide (3.85 ± 2.45 ; p value = 0.013). The partial overlap of activities of tertiary amines and anilines/amide with respect to ABCG2 alone indicated that charge cannot be a determinant for this finding. For example, the anilines **5a** and **5c** and the amide **6** are uncharged at physiological pH, but their activities are similar to those of the tertiary amines **1f** and **3**. Thus, charge of the nitrogen atom does not seem to be a criterion for interaction with ABCG2. Previous QSAR studies in ABCB1-expressing cells indicated that charge is also not a determinant for the activity of propafenone-type analogues, but that activity is determined by hydrogen bond acceptor strength in the vicinity of the nitrogen atom.^[16] If this also applies to ABCG2, SIs of anilines **5a–d** and amide **6** would be expected to be close to 0.1. In fact, they are between 1 and 10, and activities of these compounds are in the high range with respect to ABCG2. Hence, hydrogen bond acceptor strength in this part of the molecule does not seem to influence activity towards ABCG2. Two conclusions can be drawn from these findings: First, H-bond acceptor strength in the vicinity of the nitrogen atom is a major determinant for activity towards ABCB1, but most clearly not for ABCG2. Second, charge has previously been shown to be irrelevant for P-gp activity. Similarly, charge does not seem to be a determinant for ABCG2, because the activity of uncharged and charged compounds partially overlaps with respect to ABCG2. The role of the nitrogen atom was further supported by qualitative feature-based pharmacophore models. As indicated in Figure 3a and b, the pharmacophore hypothesis for ABCB1 indicates the carbonyl group and the nitrogen atom to act as H-bond acceptors (Figure 3a), whereas in the hypothesis for ABCG2 the nitrogen atom is not considered to contribute to the pharmacophore (Figure 3b). Importantly, the data set used for generation of these models was specifically selected to study the role of the nitrogen atom and not to generate pharmacophore models with general validity, such as those published previously by us and the research group of Ekins.^[9] Although the applicability of pharmacophore models for multispecific proteins such as hERG has been questioned recently, it should be noted that in the case of the ABC transporter their applicability has been demonstrated in several in silico screening attempts. This might be due to the fact that ABC transporters are considered multispecific (that is, clear SAR within congeneric series of compounds) rather than promiscuous.

QSAR studies

The remarkable difference in the SAR pattern of the two transporters encouraged us to pursue a quantitative approach in order to identify molecular descriptors that might significantly contribute to selectivity profiling attempts. Ten descriptors were selected, which had previously been proven useful in predicting ABCB1 interaction and ADME properties. These were the number of rotatable bonds (b_{1rotN}), total hydrophobic van der Waals surface area (Q_VSA_HYD), calculated $\log P$ value ($\log P$ (o/w)), molar refractivity (mr), topological polar surface area (TPSA), sum of atomic polarizabilities ($apol$), number of H-bond acceptors (a_{acc}) and donors (a_{don}), and

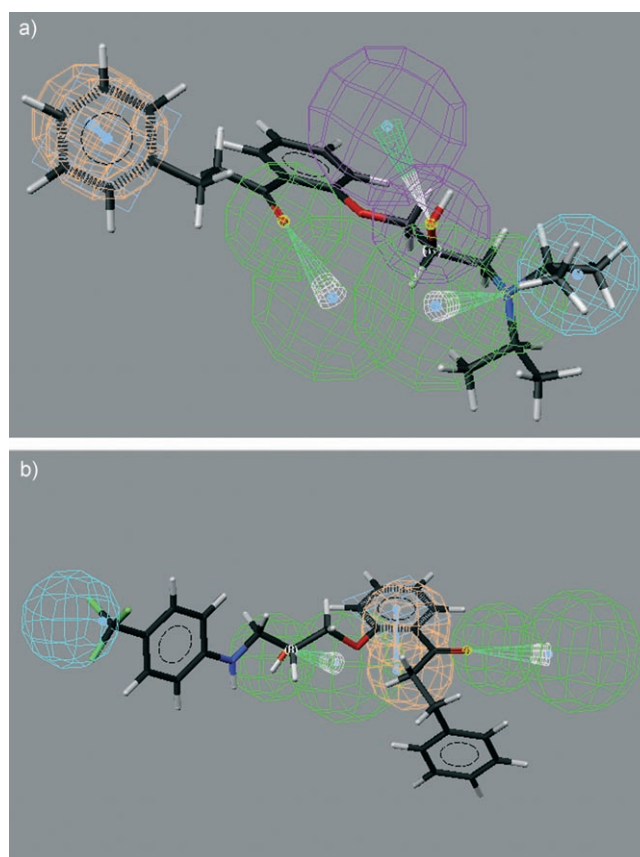


Figure 3. a) Amine **1d** mapped onto the pharmacophore hypothesis for ABCB1. Pharmacophoric features are represented as spheres and are colored according to the type of interaction; green: H-bond acceptor, blue: hydrophobic, brown: aromatic, cyan: H-bond donor. b) Aniline **5c** mapped onto the pharmacophore hypothesis for ABCG2.

the van der Waals surface area of acceptors and donors (vsa_{acc} , vsa_{don}). Final models for ABCB1 and ABCG2 were selected on the basis of highest cross-validated r^2 values and the lowest number of components as listed in Table 2.

The model for ABCB1 showed lowest r^2_{cv} , which was due to the selection of compounds according to maximal outlier characteristics with respect to the $\log P/\log$ potency ratio (4-hydroxy-4-phenylpiperidines, diphenylalkylamines, and anilines/amide). In contrast, the model for ABCG2 showed statistically significant and satisfactory predictivity with an r^2_{cv} value of 0.78. This indicates that for the class of propafenones, ABCG2

Table 2. Statistics and descriptors remaining in the QSAR models for ABCB1, ABCG2, and the SI.

Model	Descriptors ^[a]	r^2_{cv} ^[b]	rmse _{cv} ^[c]	F
ABCB1	Q_VSA_HYD, apol, vsa_acc, vsa_don, b_1rotN, a_acc	0.46	0.52	6.31
ABCG2	Q_VSA_HYD, b_1rotN, a_acc, mr	0.78	0.32	29.11
SI	Q_VSA_HYD, vsa_acc, vsa_don, b_1rotN, a_acc	0.68	0.55	16.35

[a] See the text for an explanation of descriptors. [b] r^2_{cv} : cross-validated r^2 as obtained in leave-one-out cross-validation runs. [c] rmse_{cv}: root-mean-square error as obtained in leave-one-out cross-validation runs.

is more tolerant with respect to structural variability in this set of compounds. Selectivity is therefore mainly determined by the distinct QSAR pattern with respect to ABCB1 rather than by specific interaction with ABCG2. This is not meant to imply that the design of selective ABCG2 inhibitors is not possible, as a number of highly potent ABCG2 inhibitors structurally related to the natural product FTC have been reported.^[17]

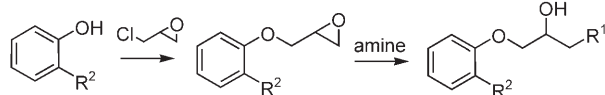
Conclusions

Herein we show that ABCB1 and ABCG2, two multispecific drug efflux pumps with overlapping substrate specificity, have defined and distinctly different feature-based interaction characteristics with propafenone analogues. The interaction of protein and drug is based on a number of molecular properties, including charge, hydrogen bonding, and hydrophobicity. Within the same chemical scaffold, selectivity indices span three orders of magnitude, demonstrating the feasibility of designing out unfavorable antitarget interactions.

Experimental Section

Design and synthesis of compounds

The design and synthesis of propafenone-type compounds has been described previously.^[14] Briefly, an appropriate hydroxyphe- none is O-alkylated with epichlorohydrin and subsequently treated with an amine to yield the respective aryloxypropanolamines (Scheme 1).



Scheme 1. Synthesis of propafenone analogues 1–6.

Cell lines

Human embryonic kidney HEK-293 cells were transfected with the pcDNA3.1 vector (Invitrogen, Carlsbad, CA, USA) containing full-length wild-type ABCG2. Stable transfectants were maintained in Eagle's minimum essential medium (Invitrogen/Gibco, Carlsbad, CA, USA) supplemented with 10% fetal bovine serum (FBS), penicillin, and streptomycin with G418 at a concentration of 2 mg mL⁻¹ as described previously.^[18] The human T-lymphoblast cell line CCRF-CEM and the P-gp-overexpressing cell line CCRFvcr1000 were provided by V. Gekeler (Altana-Pharma formerly Byk-Gulden, Konstanz, Germany). The resistant line was obtained by stepwise selection in vincristine-containing medium.^[19] Those cell lines were propagated in RPMI 1640 medium containing 10% FBS, penicillin, and streptomycin. All cells were cultured in antibiotic-free medium at least one week prior to the experiments.

Mitoxantrone steady-state accumulation experiments

The experimental protocol for determination of steady-state accumulation of mitoxantrone and daunorubicin is as follows: Cells were harvested in mid-log phase, pelleted by centrifugation at

500 g for 7 min, and resuspended on ice at a cell density of 1 × 10⁶ mL⁻¹ in RPMI 1640 medium containing 20 mM HEPES (pH 7.8), 10% FBS, and fluorescent substrate at a final concentration of 3 μM. Eight different inhibitor concentrations were prepared by serial dilution from a 100× stock solution of inhibitor in pure DMSO and added to the incubation mixture to give a final DMSO concentration of 1% (v/v). An identical concentration of DMSO was added to one tube that served as an uninhibited control. Tubes were then transferred to a 37 °C water bath and incubated for 30 min. At the end of the incubation period, cells were chilled on ice and pelleted. The supernatant was removed by aspiration, and cells were resuspended in 1 mL ice-cold culture medium. Cells were again pelleted and resuspended in 300 μL ice-cold medium. Subsequently, cell-associated fluorochrome concentration was determined in a FACScalibur flow cytometer (Becton Dickinson, San Jose, CA, USA). Hyperbolic concentration–response curves were fitted to the data points using nonlinear least squares and an iterative curve-fitting routine as implemented in the solver Add-In routine of Microsoft Excel 2002. The steady-state accumulation levels of fluorescent substrate are a function of diffusion coefficients of the compound on one hand, and the pump activity of the efflux transporter on the other. Efflux pump inhibitors increase cell-associated substrate levels, which in turn increases pump rate. Therefore, experimentally determined fluorochrome steady-state levels depend on the extent of pump inhibition and expression level of the transport protein. Expression-level-independent EC₅₀ values were calculated by considering pump-leak kinetics, which consider that a drug is both entering and leaving cells by simple diffusion, while the drug is also pumped out of the cell by a membrane-resident transport protein. For a detailed treatment of the subject, the reader is referred to the review *Kinetics of the multidrug transporter (P-gp) and its reversal* by Wilfred Stein.^[20] At least four independent experiments with eight different inhibitor concentrations were performed for each compound. Generally, experiments were repeated until a coefficient of variation of < 20% was achieved.

QSAR studies

Structures were drawn with Isis Draw and an Accord for Excel (Accelrys Inc., San Diego, CA, USA) database was generated. This was exported as an sd-file, imported into MOE (Chemical Computing Group, Montreal, Canada) and a MOE database was generated. Conversion from 2D to 3D was performed with the 3d-generator svl-script provided by the svl-exchange program from the Chemical Computing Group.

Pharmacophore modeling

The CORINA-optimized structures^[21] were imported into the modeling environment Catalyst (Accelrys Inc., San Diego, CA, USA). An automated common (qualitative) pharmacophore calculation was performed using the HipHop module of Catalyst. In the case of ABCB1 the conformational space of the pharmacophore model was given by the eight best selective compounds, and the common pharmacophore features were derived from the portion of the best five molecules (sharing the same power for selectivity), whereas the three best selective inhibitors against the ABC subtype G2 defined the conformational space and the feature constraints for the G2 pharmacophore hypothesis. Default settings were used with the following exceptions: minimum feature distance 2 Å, maximum possible conformers 600, feature weight 1.2. Allowed features were hydrophobic, hydrophobic aromatic, hydrophobic aliphatic, H-bond donor, H-bond acceptor, and ring aromat-

ic. Only hypotheses for which all training set compounds matched all conformational and feature constraints were considered further. In validation runs with the entire compound set only those for which the calculated geometric fit value was higher than the average geometric fit value for the training set were accepted as true hits.

Hansch analyses

For multiple linear regression analyses, the following descriptors were generated using the software package MOE: number of rotatable bonds (b_{1rotN}), total hydrophobic van der Waals surface area (Q_VSA_HYD), calculated log P value (log P (o/w)), molar refractivity (mr), topological polar surface area (TPSA), sum of atomic polarizabilities (apol), number of H-bond acceptors (a_{acc}) and donors (a_{don}), sum of van der Waals surface areas of H-bond acceptors and H-bond donors (vsa_{acc}, vsa_{don}). The data matrix was subject to PLS analysis using the descriptors as independent, and the respective log(1/EC₅₀) values as dependent variable. Models retrieved were further optimized via stepwise reduction of the maximum number of components followed by a variable selection procedure. The latter was performed by stepwise deletion of the least important descriptor from the input matrix. This was repeated till no further improvement of the cross-validated r^2 value was obtained.

Acknowledgements

This work was supported by grants from the Austrian Science Fund (grant 17014-B11) and the Austrian National Bank (grant 10654). The technical assistance of Manuela Hitzler is gratefully acknowledged. We thank V. Gekeler for providing us with the CCRFvcr1000 cell line.

Keywords: ABCG2 · multidrug resistance · P-glycoprotein · propafenone · selectivity profiling

- [1] J. Stefkova, R. Poledne, J. A. Hubacek, *Physiol. Res.* **2004**, *53*, 235–243.
[2] a) M. M. Gottesman, I. Pastan, *Annu. Rev. Biochem.* **1993**, *62*, 385–427;
b) S. V. Ambudkar, C. Kimchi-Sarfaty, Z. E. Sauna, M. M. Gottesman, *Oncogene* **2003**, *22*, 7468–7485.
[3] G. D. Kruh, M. G. Belinsky, *Oncogene* **2003**, *22*, 7537–7552.

- [4] L. A. Doyle, W. Yang, L. V. Abruzzo, T. Krogmann, Y. Gao, A. K. Rishi, D. D. Ross, *Proc. Natl. Acad. Sci. USA* **1998**, *95*, 15665–15670.
[5] B. J. McFarland, R. K. Strong, *Immunity* **2003**, *19*, 803–12.
[6] a) J. Yin, A. E. Beuscher 4th, S. E. Andryski, R. C. Stevens, P. G. Schultz, *J. Mol. Biol.* **2003**, *330*, 651–6565; b) M. R. Arkin, M. Randal, W. L. DeLano, J. Hyde, T. N. Luong, J. D. Oslob, D. R. Raphael, L. Taylor, J. Wang, R. S. McDowell, J. A. Wells, A. C. Braisted, *Proc. Natl. Acad. Sci. USA* **2003**, *100*, 1603–1608.
[7] D. K. Sethi, A. Agarwal, V. Manivel, K. V. Rao, D. M. Salunke, *Immunity* **2006**, *24*, 429–438.
[8] G. Cianchetta, R. W. Singleton, M. Zhang, M. Wildgoose, D. Giesing, A. Fravolini, G. Cruciali, R. J. Vaz, *J. Med. Chem.* **2005**, *48*, 2927–2935.
[9] a) S. Ekins, R. B. Kim, B. F. Leake, A. H. Dantzig, E. G. Schuetz, L. B. Lan, K. Yasuda, R. L. Shepard, M. A. Winter, J. D. Schuetz, J. H. Wikel, S. A. Wrighton, *Mol. Pharmacol.* **2002**, *61*, 964–973; b) T. Langer, M. Eder, R. D. Hoffmann, P. Chiba, G. F. Ecker, *Arch. Pharm. Pharm. Med. Chem.* **2004**, *337*, 317–327.
[10] G. F. Ecker, *Chem. Today* **2005**, *23*, 39–42.
[11] a) P. Chiba, S. Burghofer, E. Richter, B. Tell, A. Moser, G. Ecker, *J. Med. Chem.* **1995**, *38*, 2789–2793; b) P. Chiba, G. Ecker, D. Schmid, J. Drach, B. Tell, S. Goldenberg, V. Gekeler, *Mol. Pharmacol.* **1996**, *96*, 1122–1130; c) G. Ecker, P. Chiba, M. Hitzler, D. Schmid, K. Visser, H. P. Cordes, J. Csöllei, J. K. Seydel, K.-J. Schaper, *J. Med. Chem.* **1996**, *39*, 4767–4774; d) D. Schmid, G. Ecker, S. Kopp, M. Hitzler, P. Chiba, *Biochem. Pharmacol.* **1999**, *58*, 1447–1456.
[12] G. F. Ecker, K. Pleban, S. Kopp, E. Csaszar, G. J. Poelarends, M. Putman, D. Kaiser, W. N. Konings, P. Chiba, *Mol. Pharmacol.* **2004**, *66*, 1169–1179.
[13] M. Schuetzler-Muehlbauer, B. Willinger, R. Egner, G. Ecker, K. Kuchler, *Int. J. Antimicrob. Agents* **2003**, *22*, 291–300.
[14] a) G. Ecker, P. Chiba, *Recent Res. Dev. Med. Chem.* **2001**, *1*, 121–137; b) K. Pleban, G. F. Ecker, *Minirev. Med. Chem.* **2005**, *5*, 153–165.
[15] S. K. Rabindran, H. He, M. Singh, E. Brown, K. I. Collins, T. Annable, L. M. Greenberger, *Cancer Res.* **1998**, *58*, 5850–5858.
[16] G. Ecker, M. Huber, D. Schmid, P. Chiba, *Mol. Pharmacol.* **1999**, *56*, 791–796.
[17] A. van Loevezijn, J. D. Allen, A. H. Schinkel, G. J. Koomen, *Bioorg. Med. Chem. Lett.* **2001**, *11*, 29–32.
[18] R. W. Robey, Y. Honjo, K. Morisaki, T. A. Nadjem, S. Runge, M. Risbood, M. S. Poruchynsky, S. E. Bates, *Br. J. Cancer* **2003**, *89*, 1971–1978.
[19] R. Boer, V. Gekeler, W. R. Ulrich, P. Zimmermann, W. Ise, A. Schodl, S. Haas, *Eur. J. Cancer* **1996**, *32*, 857–861.
[20] W. D. Stein, *Physiol. Rev.* **1997**, *77*, 545–590.
[21] J. Sadowski, J. Gasteiger, *Chem. Rev.* **1993**, *93*, 2567–2581.

Received: July 4, 2007

Revised: October 17, 2007

Published online on November 12, 2007